Laser-induced fluorescence study of OH in flat flames of 1–10 bar compared with resonance CARS experiments

Katharina Kohse-Höinghaus, Ulrich Meier, and Brigitte Attal-Trétout

Laser-induced fluorescence (LIF) measurements of OH were performed in flat stoichiometric CH_4/air flames burning at 1, 3, 5, 7, and 9.6 bar, which had previously been investigated using OH resonance CARS. In the LIF study, line shape information and temperatures were extracted from excitation spectra; in addition, OH profiles as a function of height above the burner surface and an estimate of the OH concentration for the different flames were obtained. The perspectives and feasibility of quantitative fluorescence measurements in high pressure flames are discussed, particularly in comparison with the application of resonance CARS.
Key words: OH laser-induced fluorescence, high pressure flames, line shape parameters, temperature measurement, OH concentrations, comparison with resonance CARS.

I. Introduction

Recently, the feasibility of flame front imaging in high pressure combustion environments using laser-induced fluorescence (LIF) of OH was demonstrated.[1] There is no doubt that LIF may be applied to situations where the pressure is well above 1 bar. In this context it is of interest to evaluate the potential for quantitative measurements of temperatures and radical concentrations under such conditions and to develop suitable strategies. This would permit a comparison with flame models. For such a feasibility study, it was not advisable to investigate a technical combustion situation with 2-D radical detection. A rather simple combustion system was chosen: flat, laminar, and premixed methane/air flames were studied. Thus, problems related to rapid fluctuations of radical concentrations and their description by a flame model were avoided.

A principal advantage of LIF is that it allows one to acquire 2-D fluorescence distributions, its major drawback is that it is hampered by the loss of signal due to collisions. This is of increasing importance at high pressures. Special strategies like laser-induced predissociation fluorescence (LIPF[2]) are designed to solve the problem of variation in the quenching environment in turbulent combustion by maximizing predissociation as the dominant loss process. This is done at the cost of fluorescence intensity, and, maybe, with the additional difficulty of photodissociative production of the radical under investigation. Saturated fluorescence has also been discussed[3] for use at high pressure, although nonlinear (saturated) excitation becomes increasingly difficult with increasing pressure. It is not easy to derive quantitative concentrations from saturation techniques which can be successfully used at lower pressures.[4,5]

Resonance CARS offers a basically different alternative for the determination of radical concentrations and temperatures. It has already been applied to C_2[6] and OH[7,8] detection in combustion systems. The resonance CARS technique is not suitable for 2-D imaging, but it might be superior to LIF under conditions where this feature is not necessary. Only relative concentrations can be obtained from the resonance CARS signals. An independent calibration is required for absolute measurements. Resonance CARS is not subject to quenching. The resonance CARS signal scales with the square of the number density, meaning a high signal gain with pressure. However, this is more than compensated for by the inverse dependence of the signal on the third power of the linewidth. The linewidth itself is dependent on the chemical environment in a similarly complex fashion as the LIF signal, although the variation of the CARS signal due to this influence may be different from the one observed in LIF signals. In general, the resonance CARS experiment and theory are of a higher complexity than the LIF method. Without comparative experiments, it is

B. Attal-Trétout is with Office National d'Etudes et Recherches Aérospatiales, 92322 Châtillon, France; the other authors are with Institut für Physikalische Chemie der Verbrennung, DLR, 7000 Stuttgart 80, Federal Republic of Germany.
Received 31 July 1989.
0003-6935/90/101560-10$02.00/0.

thus hard to predict which method will offer more advantages under specific conditions. This study is an attempt to clarify the situation for one particular combustion condition.

II. Experiment

The experiment, as far as the resonance CARS study is concerned, has been described earlier.[7] Here, only the most important features are repeated. Furthermore, specific changes for the LIF experiments will be pointed out.

The laser system consisted of a pulsed Nd:YAG laser pumping a two-stage dye laser. A mixture of rhodamine 6G and fluorescein 27 produced 12 mJ near 564 nm with a 10-ns pulse duration. The dye laser light was frequency doubled to yield 1.5 mJ at 282 nm with a spectral width of 0.2 cm^{-1}. The UV radiation was separated from the dye fundamental by a UG 5 filter and three dichroic mirrors which directed the laser beam into the burner. It was thus assured that the position of the laser beam in the flame did not vary with scanning.

Premixed methane/air high pressure flat flames were stabilized on a water-cooled sintered stainless steel plate burner of 20-mm active diameter. The flame conditions are given in Table I. An annular N_2 guard flow was provided with matched flow velocities for the flames at 3 bar and above. The outer burner diameter including the shroud ring was 70 mm. The burner was mounted on a translation stage which allowed a maximum vertical adjustment of 6 mm with respect to the laser beam. Several quartz windows provided optical access for the laser and for fluorescence detection. Exhaust gases were cooled using a heat exchange unit in the top of the pressure housing. Further details concerning the burner and the stabilization of the flames have been reported elsewhere.[7]

Figure 1 shows the LIF part of the apparatus. For the excitation in the OH ($A^2\Sigma^+$–$X^2\Pi$, 1–0) band, the unfocused laser beam was used with a maximum pulse energy of 0.5 mJ. Moderate spatial resolution was provided by a pin hole 0.8 mm in diameter. The linear dependence of the fluorescence intensity on the laser power density was always ensured and controlled with neutral density filters placed in the laser beam. For detection of absorption of the laser light by the flame gases, 5% of the pulse energy was split off before the laser entered the burner. The laser intensity at this position was attenuated by suitable filters and measured with a photodiode. Similarly, a fraction of the

Table I. Flame Conditions for the Φ = 1.0 CH_4/Air Flames.[a]

p	$V(CH_4)$	V(air)	$V(N_2)$	v
bar	ℓ min^{-1}	ℓ min^{-1}	ℓ min^{-1}	cm s^{-1}
1	0.41	4.2	—	26
3	0.68	7.2	20	44
5	0.83	8.4	33	55
7	1.08	11.8	42	75
9.6	1.20	13.0	45	91

[a] The flow rates V are given for NTP conditions.

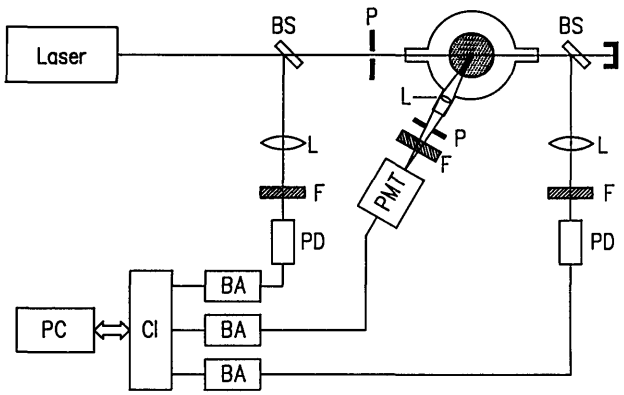

Fig. 1. Experimental setup for the LIF measurements showing the laser, the high pressure burner and the detection system. *BS*: beam splitter, *P*: pin-hole, *L*: lens, *F*: filter, *PD*: photodiode, *PMT*: photomultiplier, *BA*: boxcar averager, *CI*: computer interface, and *PC*: personal computer.

transmitted laser intensity was measured with a second, identical photodiode behind the burner. Here, a 40-mm focal length lens at a distance of two focal lengths from the photodiode moderately focused the laser light on the photodiode. This reduced considerably the beam motion on the detector caused by density fluctuations in the burner, particularly at the highest pressure.

The fluorescence signal was collected with an 83-mm focal length lens in the 17-mm bore of the burner housing, thus ensuring a comparatively large solid angle in spite of the small window size. Care was taken to avoid water condensation on the lens during the experiments. Using appropriate apertures in the fluorescence collection optics, spatial resolution in the direction of the laser beam was limited to ~5 mm in the center of the 20-mm diameter flame. With a broadband interference filter (38-nm FWHM, centered at 315 nm) the fluorescence was detected in the (1–1) and (0–0) bands with a XP2020 photomultiplier (Valvo).

Three fast boxcar averagers (Stanford Research Systems) served for the acquisition of the laser intensities monitored by the two photodiodes and the fluorescence intensity. They were interfaced to a personal computer. The detection system was triggered with scattered light from the Nd:YAG laser beam detected by a UVH 20 photocell. Typically, laser intensities and fluorescence signals were averaged for thirty laser pulses. Synchronization of the data acquisition system with the stepping motor which scanned the laser wavelength was controlled with the aid of known line positions and was accurate to 1%. For the linear excitation used here, the fluorescence signal was normalized to the laser intensity measured by the first photodiode. Absorption of the laser light in the flame was determined from the ratio of the laser intensities measured by the two photodiodes.

III. Results and Discussion

The potential of quantitative LIF measurements in flames at elevated pressures was examined. Several

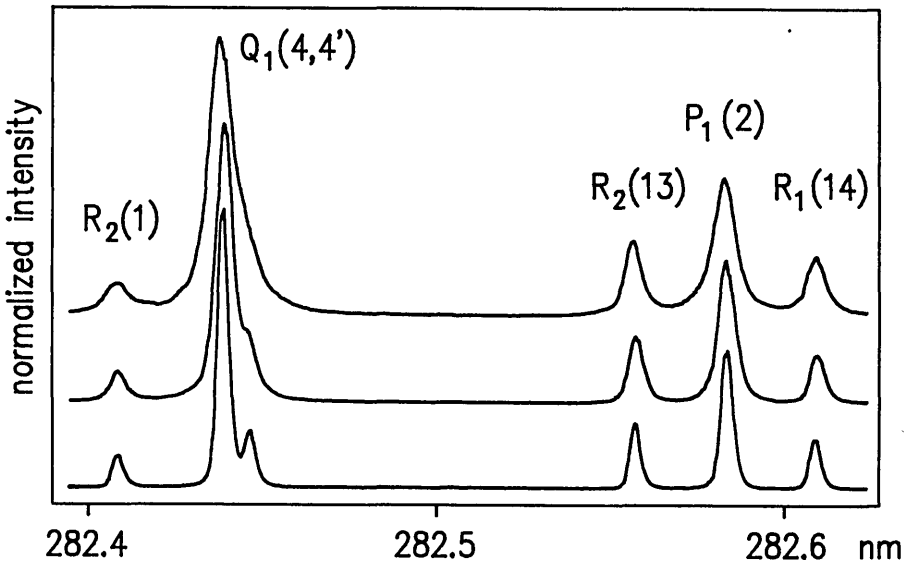

Fig. 2. OH spectra for (1–0) excitation in stoichiometric CH_4/air flames at 1 bar (bottom), 5 bar (middle), and 9.6 bar (top).

important results of these experiments will be discussed below: measurements of line shapes for the excited transition, of temperatures, of fluorescence intensities, and of OH number densities in the five flames at different pressures.

OH line shapes and rotational temperatures were obtained from excitation spectra in the (1–0) band. Figure 2 shows as an example three spectra taken at 1, 5, and 9.6 bar. Whereas the lines are quite well separated at 1 bar, they start to overlap at 9.6 bar. From spectra in this particular region of the (1–0) band, temperatures were determined. Additional line shape information was obtained from scanning a line in the (1–0) S branch.

The dependence of the fluorescence intensity on pressure was determined at different heights above the burner. Also, fluorescence intensity profiles vs height above the burner were measured for the different flames. An estimate of the OH concentration was obtained from absorption which was detected simultaneously with the fluorescence in some experiments. The possibility of partially saturating the excited transition was briefly examined at 1 and 9.6 bar.

In Sec. III. A–D, these measurements and their evaluation will be discussed.

A. Line Shapes and Pressure Broadening

The spectral overlap of the laser profile with the absorption line influences the measured fluorescence intensity. The line shape of the excited transition is subject to collisional processes and is thus pressure dependent. Line shapes in five flames at different pressures were measured and analyzed.

In the current experiments, the laser spectral width was smaller than the molecular linewidth so that line shape information for the excited transition could be obtained. For this, the $S_{21}(2)$ line was scanned in all

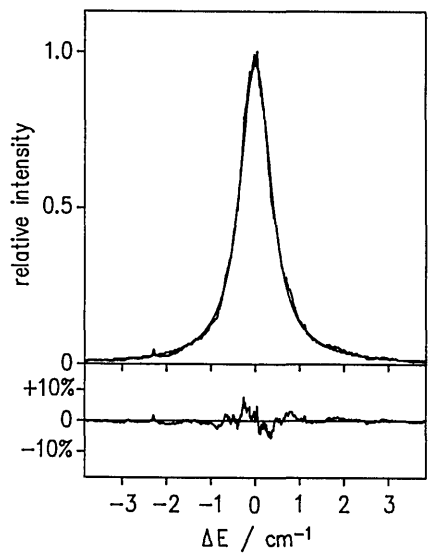

Fig. 3. OH (1–0) $S_{21}(2)$ line shape in the 9.6-bar flame at h = 6 mm. The measured line profile was fitted for T = 2000 K with a Voigt profile and a collision broadening coefficient γ = 0.040 atm^{-1} cm^{-1}. The lower panel shows the residual error of the fit.

flames in the burnt gases at 6 mm above the burner surface. The line positions in the (1–0) S branch, which offers the advantage of a wide line spacing, were assigned in recent experiments.[9,10] The lineshape analysis was performed with a program[11] which calculated a standard Voigt profile. The collisional broadening coefficient γ was used as the fitting parameter. The input temperature was in all cases chosen to be 2000 K. The adequacy of this assumption will be discussed below. With increasing pressure, an increasing influence of the collisional broadening on the line shape is expected. Figure 3 shows the measured

line shape at 9.6 bar together with the best fit. The calculated profile was obtained with a collisional broadening coefficient of $\gamma = 0.040\ \mathrm{atm^{-1}\ cm^{-1}}$. The lower panel shows the residual of the fit, the minimal least squares residual being the criterion for the best fit.

Similarly, the line shapes measured in the flames at 3, 5, and 7 bar were analyzed. The broadening coefficients γ from these fits agreed excellently with the one obtained at 9.6 bar. The results of the line shape analysis are shown in Fig. 4. The symbols give the experimental full linewidth at half maximum (FWHM), the solid line is the corresponding least squares fit, and the broken line shows the contribution of collisional broadening to the entire line shape as the product of 2γ with pressure p, using the measured γ.

For the flame at 1 bar, the influence of the laser spectral width on the $S_{21}(2)$ line shape could not be neglected. In this case, the excitation line profile was dominated by Doppler broadening and the spectral width of the laser was no longer much smaller than the linewidth. An empirical function was used to simulate the spectral shape of the laser. In very similar form, this function was applied before[7] for the line shape fitting in the resonance CARS experiments. It gives a good representation of the experimentally observed laser spectral shape with $\sim 0.2\ \mathrm{cm^{-1}}$ FWHM. The function describing the laser profile is composed of the sum of two Gaussians, one with a FWHM of $0.19\ \mathrm{cm^{-1}}$ and a relative maximum of 1.0, the other with a FWHM of $0.27\ \mathrm{cm^{-1}}$ and a relative maximum of 0.25. The second, broader Gaussian serves to make the wings of the function more realistic. This combined Gaussian function was then convolved with the Voigt profile to fit the measured line shape at 1 bar.

As shown in Fig. 4 by the circle, the inclusion of the laser spectral width allowed us to describe the line shape at 1 bar by a Voigt profile using the same collision broadening coefficient γ as for higher pressures, where the line shape was dominated by pressure broadening. The influence of the laser spectral width on the line shape at 3 bar was examined with the same procedure as for 1 bar and found to be negligible.

The temperature in the different investigated flames varied only slightly, as shall be discussed in the next section. In the burnt gases of the methane/air flames, γ is a weighted sum of the contributions of the main constituents, N_2 (~70%), H_2O (~20%), and CO_2 (~10%). These mole fractions are not expected to change much with pressure.

The pressure broadening parameter γ determined from the experimental line shapes can be compared with literature values. The broadening coefficients obtained here by measuring excitation spectra are directly comparable to those measured in absorption experiments. The broadening parameter is known[12,13] to be dependent on temperature and on the rotational quantum number N''.

From shock tube experiments[12] as well as from experiments in H_2/O_2 flames, which were doped with CO_2 in some conditions,[13] the individual broadening parameters for N_2, H_2O, and CO_2 are known at high temperatures as a function of the rotational quantum number. For these collision partners, γ shows a pronounced increase towards low N'' and levels off at higher N''. From these data, the broadening parameter for the burnt gases of the flames in this work can be estimated to be $\sim 0.034\ \mathrm{atm^{-1}\ cm^{-1}}$ for low N'', which is in quite good agreement with the measured γ of 0.040 $\mathrm{atm^{-1}\ cm^{-1}}$ for $N'' = 2$.

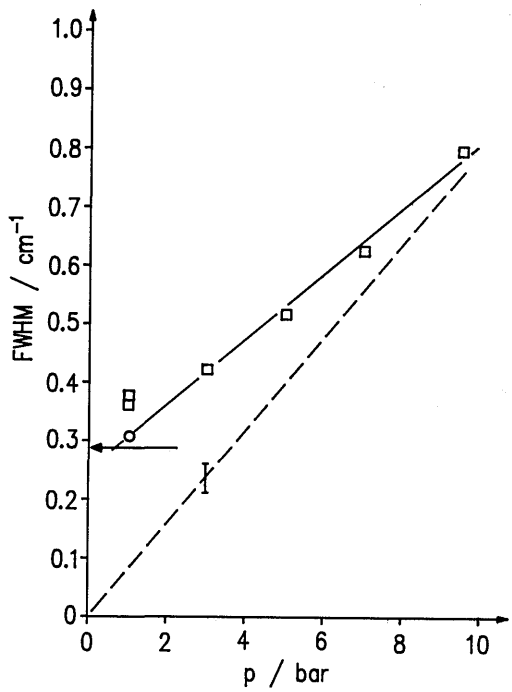

Fig. 4. Line shape analysis as a function of pressure. Squares: measured line widths (FWHM), Circle: measured FWHM at 1 bar corrected for influence of laser spectral width. Solid line: least squares fit of the measured line widths. Broken line: contribution of collisional broadening to the line widths $2\gamma \times p$; the error bar gives the uncertainty in γ. Arrow: Doppler width at 2000 K.

From spectra near 282.5 nm (like those in Fig. 2) at 9.6 bar, which were fitted using the same γ for all five lines, a slightly higher broadening parameter of 0.045 $\mathrm{atm^{-1}\ cm^{-1}}$ was obtained. This broadening coefficient is a mixture for different N''. The low N'' (1,2) with their relatively high γ are likely to contribute most to this value, making a slightly higher γ than for the isolated $S_{21}(2)$ line plausible.

In resonance CARS experiments in the same flames at the same position in the burnt gases, a collisional broadening parameter of 0.040 $\mathrm{atm^{-1}cm^{-1}}$ was obtained[7] for pumping $N'' = 7$. This γ is in good agreement with those determined from the excitation spectra. CARS line shapes are usually the result of complex interferences between terms having different spectral properties in nonlinear susceptibility.[14] However, broadening parameters can be retrieved from the spectral shape using numerical fitting, especially when a single rotational line is analyzed. The CARS line profile includes contributions from both electronic and Raman linewidths[7] which can easily be

distinguished. Obviously electronic transitions involved in the CARS susceptibility have the same linewidths as absorption transitions, which were here monitored in excitation spectra.

In previous OH absorption experiments using a narrowband dye laser,[15] an improvement of the line shape fits was noted when motional narrowing was included, as in a Galatry[16] line shape model. Transitions of OH as a diatomic hydride with large rotational level spacings are found to be susceptible to line narrowing processes dominated by soft collisions for collision partners with approximately similar masses.[15] For the experiments here, using a Galatry[11,16] instead of the Voigt profile, the line shape fitting did not lead to a significant improvement within the experimental accuracy. This was expected for the rather poor spectral resolution given by this laser in comparison with the single-mode laser in the narrowband absorption experiments.[15]

B. Temperatures

Temperatures were measured at different positions in the five flames. They were expected to be close to the adiabatic flame temperatures, which increase slightly from 2230 to 2270 K from the 1-bar flame to the 9.6-bar flame. The temperature profiles in the accessible height range from 1 to 6 mm above the burner surface should be essentially flat. The temperature gradient close to the burner surface could not be resolved. For rapid temperature determination, a region of the spectrum was chosen which offers a large energy difference within a small wavelength region. This 0.05-nm wavelength interval comprises the $R_2(13)$, $P_1(2)$, and $R_1(14)$ lines near 282.5 nm. All three lines (the right portion of the spectrum in Fig. 2) are single lines; the $R_{21}(14)$ satellite (not seen in Fig. 2) is well separated (by 0.026 nm) from the $R_1(14)$ transition. Good temperature sensitivity in the range of 1500–2500 K makes these lines well suited for the temperature determination in the methane/air flames.

All excitation spectra were measured in the linear excitation regime, where the fluorescence intensity depends linearly on the laser power density. More detailed descriptions of suitable strategies for temperature measurement in flames by LIF excitation spectra are given elsewhere;[17–19] here, only some considerations influencing the present temperature determinations shall be briefly addressed.

The key problems associated with LIF temperature measurements are polarization of the fluorescence, absorption of laser radiation by the flame gases, rotational level dependent fluorescence quantum yields due to level-specific collision efficiencies, and fluorescence trapping.

Fluorescence spectra taken in similar CH_4/air atmospheric pressure flames using the same detection system and exciting various transitions in the (1–0) band showed[19] that different directions of polarization of the laser light did not affect the measured fluorescence intensities. By exciting the (1–0) band, absorption problems can be reduced in comparison to (0–0) excitation due to the smaller Franck-Condon factor. Different amounts of laser absorption on different lines would affect the measured fluorescence intensities and thus the measured temperatures. For the three lines scanned for the temperature measurements, only the $P_1(2)$ was found to be slightly (<10%) influenced by absorption. The absorption path length for an appropriate correction of the measured fluorescence intensities was taken to be half the burner diameter, the fluorescence being observed from the flame center.

The fluorescence following (1–0) excitation was collected in the entire (1–1) and (0–0) bands. This way, effects of rotational level dependent fluorescence quantum yields[18,19] due to level-specific collision efficiencies for rotational and vibrational relaxation could be minimized, as the fluorescence of OH molecules having undergone rotational or vibrational relaxation did not escape detection. The influence of rotational level dependent quenching on the measured fluorescence intensities is less important in low pressure flames[17] if a short detection time interval early after the end of the laser pulse is used. Then the excited OH has experienced only few collisions. This was not possible here at atmospheric and higher pressures where the effective collisional lifetime was on the order of or shorter than the laser pulse duration. Quenching problems were, however, not expected to be severe, as the rotational level dependence of OH quenching by H_2O, one of the most important quenchers in these flames, seems to decrease strongly at high temperatures.[20]

Fluorescence trapping (the absorption of fluorescence light by OH molecules in the flame which are in appropriate rotational and vibrational states) in the (1–1) band was negligible due to the small population in $v'' = 1$. In the (0–0) band, where fluorescence trapping is likely to occur, the fluorescence spectra[19] showed almost no memory of the originally excited rotational level in $v' = 1$; in addition, the ratio of (1–1) to (0–0) fluorescence was very similar for different excited transitions. Being almost independent of the excited rotational level in $v' = 1$, fluorescence trapping did not cause problems for the present temperature measurements.

In the flame at 1 bar, a temperature of 2040 ± 50 K was measured independent of position. This agrees well with measurements in similar flames using CARS and Raman techniques[21] or absorption[22] and LIF spectra.[18,19] In the latter investigation,[19] temperatures measured from LIF excitation spectra with the same method as used here were checked against CARS and Raman temperatures under exactly the same flame conditions. Very good agreement was found.

In the flame at 5 bar, a temperature of 2070 ± 60 K was obtained. The spectrum at 9.6 bar indicates already some overlap in the wings of the lines due to pressure broadening (see Fig. 2). It is thus questionable whether evaluation of temperatures at 9.6 bar is still possible without fitting the entire spectrum. This was examined by calculating the spectrum from known molecular quantities[23–25] using the collisional broad-

ening parameter and the temperature as fitting parameters.

The result is shown in Fig. 5, where the measured spectrum and the best fit are shown together with the residual. A temperature of 2275 ± 70 K was obtained from this fit which is 50 K lower than determined from the line maxima. The best γ obtained by this procedure turned out to be 12% higher than the one determined from the S line shape. A potential explanation for this was given in the previous section. With this collision broadening coefficient, simulated spectra for the wavelength interval in Fig. 2 at even higher pressure exhibited some residual structure at 30 bar and two unstructured regions of completely merged lines at 100 bar. At such high pressures, the chosen wavelength region would therefore no longer be suitable for temperature measurements. The simulation of the S branch spectrum showed that these lines will remain isolated enough even at 100 bar to permit determination of the temperature. Experience with temperature measurements in the (1,0) S branch was obtained in flames at low and atmospheric pressure.[18]

In summary, the temperatures were found to be close to the adiabatic temperature. They increase moderately with pressure. From the resonance CARS experiments,[7] a temperature of 2200 ± 100 K was determined 3 mm above the burner surface for the flames at all different pressures. Regarding the overall experimental errors for both experiments, the agreement is satisfactory. A maximum temperature difference of ~200 K between the flames at the highest and lowest pressure has only a minor effect of <10% (which corresponds to the experimental accuracy) on the line shapes discussed in the previous section.

Cross-checks against CARS and Raman temperature measurements in very similar stoichiometric CH_4/air flames at 1 bar as well as a comparison with literature data[22] for such flames give additional confidence in the temperature measurements by LIF excitation spectra presented here.

C. Fluorescence Intensity Profiles

The fluorescence intensity upon excitation of $P_1(1)$ or $S_{21}(2)$ was measured as a function of pressure and of position above the burner surface. Figure 6 gives the dependence of the fluorescence intensity on the height h above the burner surface for all five flames. These intensities were only corrected for the fraction of the solid angle being obscured by the burner for the different positions. Several trends are observed. The fluorescence intensity at 1 bar has its maximum close to 0.5 mm and decreases with h. Similarly, the fluorescence intensity in the 3-bar flame shows some dependence on position, whereas the profiles are rather flat for the three flames at the highest pressures. Such behavior would be expected, as the flame front is located at different positions for the different flames. In the 1-bar flame, the flame chemistry is spread out to a much larger extent than in the flames at higher pressure. Roughly, the fluorescence intensity decreases with increasing pressure.

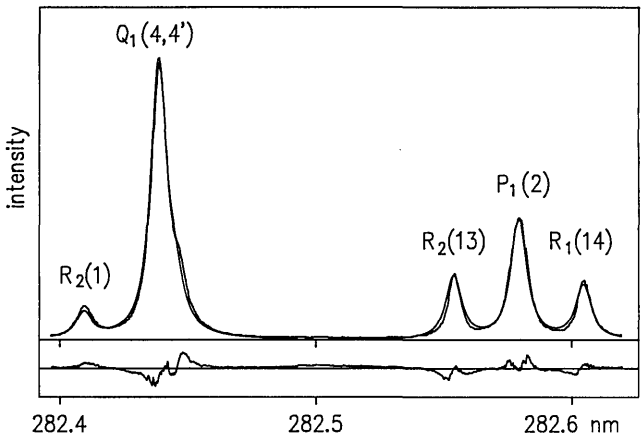

Fig. 5. Temperature determination from a spectrum at 9.6 bar. From the best fit, a temperature of 2275 ± 70 K was determined, whereas from the line maxima, 2325 ± 70 K was obtained. The lower panel shows the residual error of the fit.

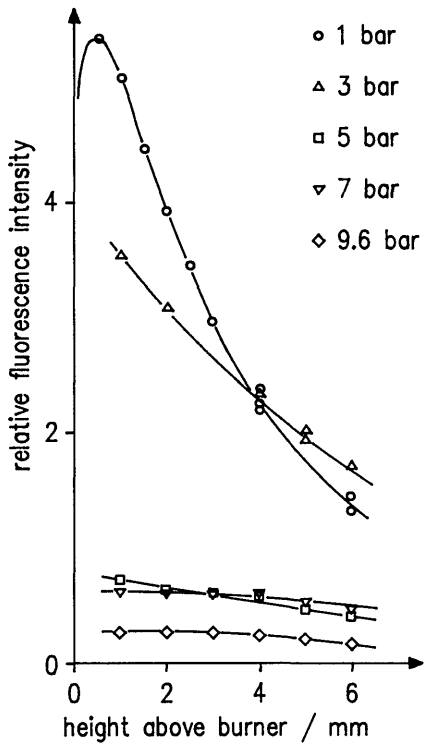

Fig. 6. Fluorescence intensity for $P_1(1)$ excitation vs height above the burner surface for the five flames at different pressures.

Figure 7 shows the fluorescence intensity at two fixed heights for the five different flames. These curves do not merely represent the pressure dependence of the fluorescence intensity, but rather a cross section through flame zones whose chemistry is in different states of evolution for each flame at the two fixed positions. It is thus hard to predict the loss of fluorescence intensity with pressure from such curves without knowing the respective OH concentrations.

Several parameters influencing the fluorescence intensity have to be considered in order to place the

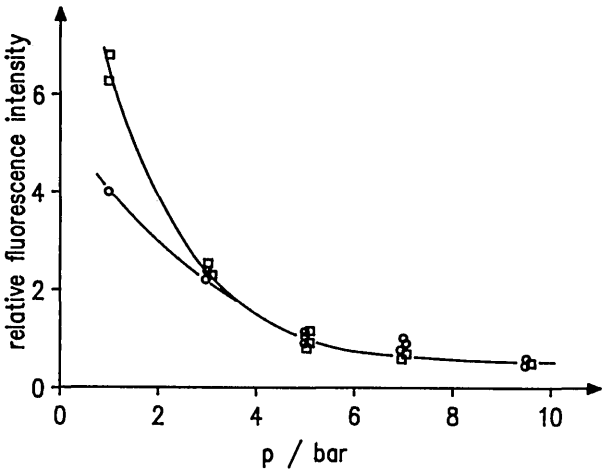

Fig. 7. Fluorescence intensity for $S_{21}(2)$ excitation vs pressure at 3 mm (squares) and 6 mm (circles) above the burner surface.

measured intensity curves in Figs. 6 and 7 on a relative or absolute concentration scale. They are briefly discussed in the following.

For intensities measured at different temperatures, the Boltzmann fraction of the ground state has to be considered. With approximately flat temperature profiles, as shown in the previous section, this is not a problem even for measurements using excitation of moderately temperature-dependent levels. The maximum temperature difference on the order of 200 K between the different investigated flames leads to a difference in Boltzmann fraction of ~10%.

Absorption of the laser light on its path through the flame was mentioned before as a potential parameter of influence on the fluorescence intensity. The absorption was measured for h = 1 and 6 mm for all flames. Some absorption [between 8 and 18% for the $P_1(1)$ line] was noticed at every condition, the differences being rather small within the experimental accuracy. In principle, the absorption can be exactly taken into account as well as the differences in Boltzmann fraction in order to evaluate relative or absolute OH concentrations. Because a final evaluation would require additional data on collisional efficiencies, as discussed below, it was not attempted to correct the fluorescence intensity profiles. The measured absorption was used instead for an estimate of the OH concentration, as shown in the next section.

The change of collision efficiency with different flame conditions is a very important aspect in the correct scaling of the fluorescence intensity curves as concentration profiles. Collisions have two effects which may both influence the fluorescence signal. First, they broaden the absorption line, and second, they change the fluorescence quantum yield.

The first effect leads to a changing overlap of the laser spectral profile and the absorption line with pressure. For this particular experiment, the fluorescence intensity was always measured with the laser positioned at the center of the excited line, and, under all conditions, the spectral width of the laser was smaller than the line width. Thus the influence of the laser spectral width on the fluorescence intensity curves in Figs. 6 and 7 was insignificant even at 1 bar where the absorption line was not much broader than the laser spectral profile. For the evaluation of OH concentrations from the fluorescence signals in Figs. 6 and 7, however, the change in the fraction of absorbing molecules with pressure, caused by the broadening of the absorption line by collisions, would need to be considered.

The second effect of collisions is the change of fluorescence quantum yield with pressure and with position in the flame. The collision efficiency is dependent on chemical environment, temperature, and pressure, as well as on the rotational quantum number. Correcting the fluorescence intensities appropriately thus requires a wealth of detailed information which is at present just partly available. With a picosecond laser, the effective lifetime at every flame condition could be measured to yield this information. At 1 bar, the effective fluorescence lifetime was ~1.9 ns, as measured with a picosecond laser in a very similar stoichiometric CH_4/air flame.[26] At higher pressures, no lifetime data are currently available. In the present experiment, the laser pulse duration (~10 ns) was always much longer than the effective fluorescence lifetime.

Although the fluorescence intensities are related to the OH concentrations in a rather complex way, some qualitative observations are possible for the present measurements. In the flames at the higher pressures (5–9.6 bar), the concentrations of the most efficient colliders (H_2O, CO_2, and N_2) are likely to be almost independent of position for heights between 1 and 6 mm. Also, the mole fractions for these colliders are probably not much different for these flames which burned at the same stoichiometry, but at different pressures. Under these conditions, the individual fluorescence profiles at the higher pressures therefore most likely represent relative concentration profiles. The situation is different for the 1-bar flame where the poorer quencher N_2, of course, does not vary much throughout the flame, but where the more effective ones, H_2O and CO_2, attain their respective maxima only at greater distances from the burner surface.

D. OH Concentrations

A crude concentration estimate can be obtained from the measured absorption at the two positions in the five flames. The result for the 1-bar flame is shown in Fig. 8. The broken line is the fluorescence intensity profile from Fig. 6. The filled circles are absolute concentrations evaluated from the measured absorption. For a comparison, the solid line gives an absolute OH concentration profile which was measured by Cattolica[22] using absorption in a very similar stoichiometric CH_4/air flame. The agreement between the two estimated concentrations (believed to be accurate to ~30%) and the result of Cattolica[22] is excellent. The shape of the fluorescence intensity profile is clearly different from that of the concentra-

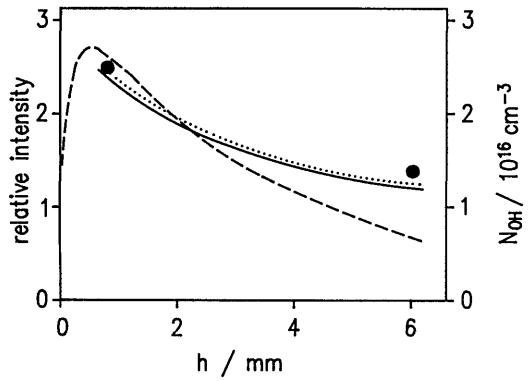

Fig. 8. Fluorescence intensity and OH number density at 1 bar. Broken line: measured fluorescence intensity for $P_1(1)$ excitation (left ordinate). Circles: OH number densities from measured absorption; dotted line: OH number density from resonance CARS experiments[7] (scaled with known OH equilibrium concentration at h = 6 mm); solid line: OH number density from absorption in a very similar flame[22] (right ordinate for all curves).

tion profile. Reasons for this have been discussed above. Included in this comparison in Fig. 8 is the OH concentration profile obtained from the resonance CARS measurements[7] as the dotted line; the corresponding relative OH concentrations were placed on an absolute scale (within 30% accuracy) using the equilibrium OH concentration for the 1-bar flame at $h = 6$ mm as reference. The agreement with the absorption data is excellent, but should not be overinterpreted considering the error sources in both experiments.

The OH number density was also determined for the flames at higher pressures. It was again estimated from the measured absorption. With increasing pressure, decreasing mole fractions of OH, but very similar number densities were found. For example, at 9.6 bar and $h = 6$ mm, the measured absorption yielded a number density of $3.9 \times 10^{16}/\text{cm}^3$ in comparison with $4.0 \times 10^{16}/\text{cm}^3$ from the resonance CARS experiment.[7] This is about a factor of 3 higher than the number density of $1.4 \times 10^{16}/\text{cm}^3$ estimated from absorption and of $1.2 \times 10^{16}/\text{cm}^3$ obtained from the resonance CARS experiment[7] in the 1-bar flame at the same height of $h = 6$ mm. The relative concentrations evaluated from the resonance CARS measurements were again placed on an absolute scale using the assumed OH equilibrium concentration at 1 bar, $h = 6$ mm as reference.

A simulation of the flame at 1 bar with a numerical model[27] gave number densities of $2.3 \times 10^{16}/\text{cm}^3$ at $h = 1$ mm and of $1.2 \times 10^{16}/\text{cm}^3$ at $h = 6$ mm in very good agreement with the measured values. The simulation excellently reproduced the shape of the measured OH concentration profile. For the flame at 9.6 bar, the numerical simulation had a more preliminary character; here, an OH concentration of $6.5 \times 10^{16}/\text{cm}^3$ was obtained for $h > 2$ mm. The agreement between the concentrations calculated with the flame model and the concentrations estimated from the absorption and resonance CARS experiments[7] is better than a factor of 2, thus lending a solid foundation to the qualitative trends concluded from this study of flames at different pressures.

One interesting aspect for the extension of the pressure range in further studies is the signal-to-noise ratio S/N. For excitation in the S branch of the (1–0) band, the S/N at 9.6 bar was >25 (when averaging 30 shots), the detection system not yet being fully optimized. The Einstein A coefficients are more than a factor of 20 more favorable for the (1–0) P, Q, and R lines, corresponding to a S/N of ~500. A factor of ~4 could additionally be gained by using (0–0) band excitation. Of course, potential problems with absorption of the laser light should be kept in mind for (0–0) excitation.

The net loss of fluorescence signal with pressure is an interesting quantity in this context as it allows one to estimate the OH detection limit. The OH number density at $h = 6$ mm is a factor of ~3 higher in the flame at 9.6 bar than in the flame at 1 bar. The measured loss of fluorescence signal between the two flames at 1 and 9.6 bar at $h = 6$ mm is a factor of ~6. Assuming the number density to be kept constant at its value at 1 bar and $h = 6$ mm, the net signal loss would then be a factor of ~18. This incorporates the signal loss caused by quenching as well as the loss due to the increase in the width of the absorption line with pressure. The fluorescence signal loss approximately matches the increase in quenching of a factor of ~10 times the increase in absorption line width of a factor of 2.6. Between 10 and 100 bar, the absorption line width will broaden due to collisions by a factor of ~10; also, the quenching will increase by an order of magnitude. Thus the fluorescence signal loss will be a factor of ~100. With the present S/N in the (1–0) P, Q, and R branches of 500, the detection of OH seems therefore possible also in flames at 100 bar, given the same OH number density as in the flame at 1 bar.

Similarly, the pressure range for the applicability of the resonance CARS detection of OH can be estimated. The S/N obtained for the $O_{12}^{(1-0)}(7)$,$P_1^{(0-0)}(7)$, $P_1^{(1-0)}(7)$ triple resonance CARS line at 9.6 bar was ~30, which was measured with a smaller laser pulse energy than achievable with the present laser system.[7] Normalizing to the density at 1 bar, this would correspond to S/N = 1 at ~20 bar. Flames at pressures up to 100 bar might be studied with improved background rejection and a ten times higher laser energy for each of the laser beams generating the CARS signal.

IV. Conclusions

OH line shapes, rotational temperatures, and concentrations have been obtained in flames burning at 1–9.6 bar. The results give a good basis for the discussion of appropriate LIF measuring strategies with the aim of quantitative measurements. The problems connected with accurate temperature and concentration measurements are about the same as at 1 bar. As expected, the fluorescence signal loss corresponds to the increase in quenching collisions and broadening of the absorption line under the assumption of similar

number densities. The S/N is good enough to allow measurements in similar flames at higher pressures.

Up to 9.6 bar, the spectra show structure similar to those at 1 bar. With the measured collision broadening coefficient, simulations for higher pressures (30–100 bar) indicate that different strategies must be applied for temperature measurements. For sufficiently high fluorescence intensities, (1–0) S lines could be used; another possibility would be the evaluation of intensity ratios for different spectral regions similar to the rapid fitting schemes used in the determination of CARS temperatures.[28]

For OH concentration measurements at higher pressures, calibration by absorption would be possible in the same way as was demonstrated here. However, such an independent calibration would not be necessary, if the collision efficiencies were known for the pressures and flame positions of interest. Effective lifetime could be measured with a picosecond laser system. Furthermore, numerical modeling of the collisional quenching and energy transfer processes on the basis of the currently available, yet incomplete, set of rate coefficients employing suitable scaling and fitting laws could be used to simulate the influence of collisions on the fluorescence intensities for different flame compositions and pressures. Such models[29,30] have been developed for similar purposes and would have to be actualized.

Predissociation LIF (LIPF) has been discussed[3] as a collision-insensitive technique for OH concentration measurements in high pressure combustion systems. This method might suffer from a severe loss of fluorescence intensity at high pressures, as the predissociation (which does not lead to fluorescence) must always dominate the effective rate of collisions. The same idea of reducing the influence of collisions by making a different process dominant is followed with nonlinear (saturated) excitation schemes,[4–6] which in contrast lead to particularly high fluorescence intensities. The feasibility of both LIPF and saturated LIF has not yet been demonstrated in flame experiments at high pressures. In a preliminary experiment at rather low laser power density, where only a very moderate saturation degree was measured in the 1-bar flame, saturation was not achieved at 9.6 bar. This experiment will be repeated with a higher laser power density.

In comparison with LIF, data of similar quality is obtained from resonance CARS measurements of OH.[7] Temperatures can be determined by resonance CARS using a slight detuning of one of the laser frequencies. This method is applicable at any pressure provided the signal is strong enough. Relative concentrations can be evaluated from resonance CARS signals as soon as collisional effects on the line shapes are known. An independent calibration is necessary to place these concentrations on an absolute scale; here, the equilibrium OH concentration in the burnt gases was used for this purpose. The measured signal-to-noise ratio is similar for both LIF and resonance CARS and permits to extrapolate the range of applicability to 30–100 bar. Neither method seems to be totally superior for OH concentration and temperature measurements in high pressure combustion situations. Depending on the particular application, resonance CARS might be chosen because of its coherent nature, or LIF because of its 2-D imaging capabilities.

The authors would like to thank Jean-Pierre Taran and Thomas Just for their interest in this study. They are grateful to Philippe Dumas for participating in some of the experiments, to Annette Lawitzki for helping with part of the data evaluation and to Siegfried Kelm for performing some flame model calculations. Also, they would like to thank Jürgen Warnatz for a copy of his current flame code.

References

1. R. Suntz, H. Becker, P. Monkhouse, and J. Wolfrum, "Two-Dimensional Visualization of the Flame Front in an Internal Combustion Engine by Laser-Induced Fluorescence of OH Radicals," Appl. Phys. **B47**, 287–293 (1988).
2. P. Andresen, A. Bath, W. Gröger, H. W. Lülf, G. Meijer, and J. J. ter Meulen, "Laser-Induced Fluorescence with Tunable Excimer Lasers as a Possible Method for Instantaneous Temperature Field Measurements at High Pressure: Checks with an Atmospheric Pressure Flame," Appl. Opt. **27**, 365–378 (1988).
3. C. D. Carter, J. T. Salmon, G. B. King, and N. M. Laurendeau, "Feasibility of Hydroxyl Concentration Measurements by Laser-Saturated Fluorescence in High-Pressure Flames," Appl. Opt. **26**, 4551–4562 (1987).
4. K. Kohse-Höinghaus, R. Heidenreich, and T. Just, "Absolute Concentration Measurements of OH in Low-Pressure Hydrogen–Oxygen, Methane–Oxygen, and Acetylene–Oxygen Flames," *Twentieth Symposium (International) on Combustion* (Combustion Institute, Pittsburgh, USA, 1984) p. 1177.
5. R. P. Lucht, D. W. Sweeney, and N. M. Laurendeau, "Laser-Saturated Fluorescence Measurement of OH Concentrations in Flames," Combust. Flame **50**, 189–205 (1983).
6. B. Attal, D. Débarre, K. Müller-Dethlefs, and J. P. E. Taran, "Resonance-Enhanced Coherent Anti-Stokes Raman Scattering in C_2," Revue Phys. Appl. **18**, 39–50 (1983).
7. B. Attal-Trétout, S. C. Schmidt, E. Crété, P. Dumas, and J. P. Taran, "Resonance CARS of OH in High-Pressure Flames," to appear in J. Quant. Spectrosc. Radiat. Transfer, Mar. 1990.
8. B. Attal-Trétout and P. Bouchardy, "Detection of the OH Radical in Flames by Resonance CARS," Rech. Aérosp. 19–38 (**1987–5**).
9. S. R. Lin, S. T. Lee, and Y. P. Lee, "The S_{21} Lines of the $A^2\Sigma^+$ (v' = 1) ← $X^2\Pi$ (v'' = 0) Transition of OH and OD," J. Quant. Spectrosc. Radiat. Transfer **38**, 163–166 (1987).
10. R. Tirgrath, "Bestimmung von OH-Konzentrationen und Rotationstemperaturen in Stationären und Instationären Unterdruckflammen mit Laser-Induzierter Fluoreszenz," Thesis, DLR Stuttgart, in preparation.
11. Program based on the approach used in P. L. Varghese, Thesis, "Tunable Infrared Diode Laser Measurements of Spectral Parameters of Carbon Monoxide and Hydrogen Cyanide," Stanford University (1983).
12. E. C. Rea, Jr., A. Y. Chang, and R. K. Hanson, "Shock-Tube Study of Pressure Broadening of the $A^2\Sigma^+$–$X^2\Pi$ (0,0) Band of OH by Ar and N_2," J. Quant. Spectrosc. Radiat. Transfer **37**, 117–127 (1987).
13. E. C. Rea, Jr., A. Y. Chang, and R. K. Hanson, "Collisional Broadening of the $A^2\Sigma^+$ ← $X^2\Pi$ (0, 0) Band of OH by H_2O and CO_2 in Atmospheric-Pressure Flames" J. Quant. Spectrosc. Radiat. Transfer **41**, 29–42 (1989).

14. B. Attal-Trétout, P. Berlemont, and J. P. E. Taran, to appear in Molec. Phys., April 1990.
15. E. C. Rea, Jr., A. Y. Chang, and R. K. Hanson, "Motional Narrowing Effects in Spectral Line Profiles of OH," submitted for publication.
16. L. Galatry, "Simultaneous Effect of Doppler and Foreign Gas Broadening on Spectral Lines," Phys. Rev. **122,** 1218–1223 (1961).
17. K. J. Rensberger, J. B. Jeffries, R. A. Copeland, K. Kohse-Höinghaus, M. L. Wise, and D. R. Crosley, "Laser-Induced Fluorescence Determination of Temperatures in Low Pressure Flames," Appl. Opt. **28,** 3556–3566 (1989).
18. A. Lawitzki, R. Tirgrath, U. Meier, K. Kohse-Höinghaus, A. Jörg, and T. Just, "Temperature Measurements in Flames by Linear and Non-Linear Laser-Induced Fluorescence," in *Proceedings of the Joint Meeting of the German and Italian Sections of the Combustion Institute*, Ravello, Italy, Sept. 11–14, 1989, paper 1.4.
19. A. Lawitzki, I. Plath, W. Stricker, J. Bittner, U. Meier, and K. Kohse-Höinghaus, "Laser-Induced Fluorescence Determination of Flame Temperatures in Comparison with CARS Measurements," submitted for publication.
20. J. B. Jeffries, K. Kohse-Höinghaus, G. P. Smith, R. A. Copeland, and D. R. Crosley, "Rotational Level Dependent Quenching of $OH(A^2\Sigma^+)$ at Flame Temperatures," Chem. Phys. Lett. **152,** 160–166 (1988).
21. W. Stricker and M. Woyde, "CARS Temperature Measurements in High Pressure Flames," in *Proceedings of the Joint Meeting of the German and Italian Sections of the Combustion Institute*, Ravello, Italy, Sept. 11–14, 1989, paper 1.1.
22. R. J. Cattolica, "OH Radical Nonequilibrium in Methane–Air Flat Flames," Combust. Flame **44,** 43–59 (1982).
23. G. H. Dieke and H. M. Crosswhite, "The Ultraviolet Bands of OH," J. Quant. Spectrosc. Radiat. Transfer **2,** 97–199 (1962).
24. I. L. Chidsey and D. R. Crosley, "Calculated Rotational Transition Probabilities for the *A–X* System of OH," J. Quant. Spectrosc. Radiat. Transfer **23,** 187–199 (1980).
25. M. R. Trolier, "Kinetic and Spectroscopic Studies of Ozone Photochemistry," Thesis, Cornell U., Ithaca, NY, (1988).
26. M. Köllner, P. Monkhouse, and J. Wolfrum, to be published.
27. J. Warnatz, "The Structure of Laminar Alkane-, Alkene-, and Acetylene Flames," *Eighteenth Symposium (International) on Combustion* (Combustion Institute, Pittsburgh, 1981), p. 369.
28. A. C. Eckbreth, G. M. Dobbs, J. H. Stufflebeam, and P. A. Tellex, "CARS Temperature and Species Measurements in Augmented Jet Engine Exhausts," Appl. Opt. **23,** 1328–1339 (1984).
29. D. H. Campbell, "Collisional Effects on Laser-Induced Fluorescence Measurements of Hydroxyl Concentrations in a Combustion Environment. I. Effects for $v' = 0$ Excitation," Appl. Opt. **23,** 689–703 (1984).
30. D. H. Campbell, "Collisional Effects on Laser Induced Fluorescence Measurements of Hydroxyl Concentrations in a Combustion Environment. 2: Effects for $v' = 1$ Excitation," Appl. Opt. **23,** 1319–1327 (1984).